Effect of Random and Block Copolymer Additives on a Homopolymer Blend Studied by Small-Angle Neutron Scattering

GRETCHEN VOGE,[1,*] KARI FOSSER,[1,†] DEAN WALDOW,[1] ROBERT BRIBER,[2] ADEL HALASA[3]

[1]Department of Chemistry, Pacific Lutheran University, Tacoma, Washington 98447

[2]Department of Materials Science and Engineering, University of Maryland, College Park, Maryland 20472

[3]Corporate Research Division, Goodyear Tire and Rubber Company, 142 Goodyear Boulevard, Akron, Ohio 44305

Received 2 September 2003; revised 9 February 2004; accepted 9 February 2004
DOI: 10.1002/polb.20184
Published online in Wiley InterScience (www.interscience.wiley.com).

ABSTRACT: Small-angle neutron scattering (SANS) has been employed to study a blend of polystyrene and polybutadiene modified by copolymer additives. SANS data from the one-phase region approaching the phase boundary has been acquired for blends modified by random and diblock copolymers that have equal amounts of styrene and butadiene monomers as well as a random copolymer with an unequal monomer composition. The binary blend is near the critical composition, and the copolymer concentrations are low at 2.5% (w/w). The data have been fitted with the random-phase approximation model (binary and multicomponent versions) to obtain Flory–Huggins interaction parameters (χ) for the various monomer interactions. These results are considered in the context of previous light scattering data for the same blend systems. The SANS cloud points are in good agreement with previous results from light scattering. The shifts in the phase boundary are due to the effects of the additives on the χ parameter at the spinodal. All the additives appear to lower the χ parameter between the homopolymers; this is in conflict with the predicted Flory–Huggins behavior. © 2004 Wiley Periodicals, Inc. J Polym Sci Part B: Polym Phys 42: 3191–3203, 2004

Keywords: additives; blends; block copolymers; compatibilization; miscibility; neutron scattering; phase behavior; phase separation; thermodynamics

INTRODUCTION

Polymer blends constitute a significant portion of industrial polymer production and hold great academic interest. The alloying of commodity polymers into blends has become very common and is often effective in producing high-performance materials.[1–3] The low miscibility of polymer blends has led to extensive research into their thermodynamic and kinetic properties and the development of many additives used to overcome poor miscibility. A common method of improving poor miscibility is to add a third component to a blend that will have a favorable interaction with the precursor polymers. Diblock, graft, random, and other copolymer additives have been studied to determine how they affect various aspects of blend systems. Adding copolymers with different

**Present address:* University of Maryland School of Medicine, Baltimore, Maryland 21201

†*Present address:* Department of Chemistry, University of Illinois at Urbana–Champaign, Urbana, Illinois 61801

Correspondence to: D. Waldow (E-mail: waldow@chem.plu.edu)

Journal of Polymer Science: Part B: Polymer Physics, Vol. 42, 3191–3203 (2004)

structures and monomer compositions may change the range of miscibility, the interfacial strength of separated domains, and the morphology of separated domains. A long-term goal of much of the research on polymer blends is the determination of how the structure and monomer composition of a copolymer can affect the thermodynamics and kinetics of phase separation.

Barham et al.[4] used wide-angle light scattering to study the polystyrene (PS)/polybutadiene (PB) polymer system and the role of three different copolymer additive architectures: random and diblock copolymers with equal monomer compositions and a random copolymer with an unequal monomer composition. In their study, the PS/PB blend with either a random copolymer (50/50 monomer content) or diblock copolymer (50/50 monomer content) added was able to lower the temperature of the phase boundary. On the other hand, the random copolymer with an unequal monomer composition (20/80 monomer content) resulted in an increase in the phase-separation temperature, and this destabilized the system. Their kinetics results indicated that all three copolymers were able to slow the phase-separation rates in these systems. These results were interesting because in previous studies[5–9] in which copolymer additives were observed to stabilize a blend system, the phase-separation kinetics were also slowed. This slowdown is usually attributed to the copolymer additive migrating to the interface and thus lowering the interfacial energy between phases. The lower interfacial energy is related to the reduction in the effective Flory–Huggins parameter (χ) because of the added copolymer. Barham et al. also observed that an asymmetric composition random copolymer destabilized the phase boundary and yet slowed phase-separation kinetics. Generally, if the phase boundary moves to higher temperatures for an upper critical solution temperature (UCST) system, it is associated with an effective increase in the χ parameter. If the effective χ parameter does indeed increase, then this conclusion is in conflict with the argument for slower phase separation due to lower interfacial energy.

To better understand these effects, small-angle neutron scattering (SANS) has been used to study the same PS/PB polymer system except with deuterated polystyrene (d8PS). This approach allows a more complete picture of the thermodynamic parameters and complements the previous light scattering data. SANS experiments were conducted on a binary d8PS/PB blend with and without the following copolymers: a random copolymer with an equal monomer composition, a random copolymer with an unequal monomer composition, and a diblock copolymer with an equal monomer composition. The concentrations of the added copolymers were low and substantially away from the anticipated bicontinuous microemulsion region.[10–14] A multicomponent mean-field random-phase approximation (RPA) theory is presented in the next section and is used to analyze the SANS data in this article. Deviations from the mean field in the inverse susceptibility data have been a subject of discussion in recent literature for similar systems.[15–21] This article focuses on the development and application of ternary mean-field RPA analysis. As such, the applicability of RPA is strictly valid at temperatures well away from the phase transition. Deviations from the mean field are interesting and will be the focus of future work but are beyond the scope of this article.

SCATTERING THEORY

The SANS analysis method for multicomponent polymer blends presented here follows the block $n + 1$ matrix method of Akcasu and others.[22–25] The measured structure factor $I(q)$ (where q is the wavevector) is related to the multicomponent structure factor $\mathbf{S}(q)$:

$$I(q) = \mathbf{B}^T\mathbf{S}(q)\mathbf{B} \tag{1}$$

where vector $\mathbf{B}$ and its transpose contain the scattering contrast factors for the components. The multicomponent structure factor is defined as follows:

$$\mathbf{S}(q) = \left[\frac{1}{\mathbf{S}^o(q)} + \mathbf{V}(q)\right]^{-1} \tag{2}$$

where $\mathbf{S}^o(q)$ contains the bare structure factors and all interaction parameters are contained in $\mathbf{V}(q)$. These equations are applied in three cases: (1) a binary blend (a two-component system), (2) a binary blend with an added random copolymer (a three-component system), and (3) a binary blend with an added diblock copolymer. For case 3, the two blocks of the diblock are treated as individual components, and this makes this blend a four-component system (see Fig. 1 for a schematic of these cases, including specific definitions of the components and their respective interactions). In

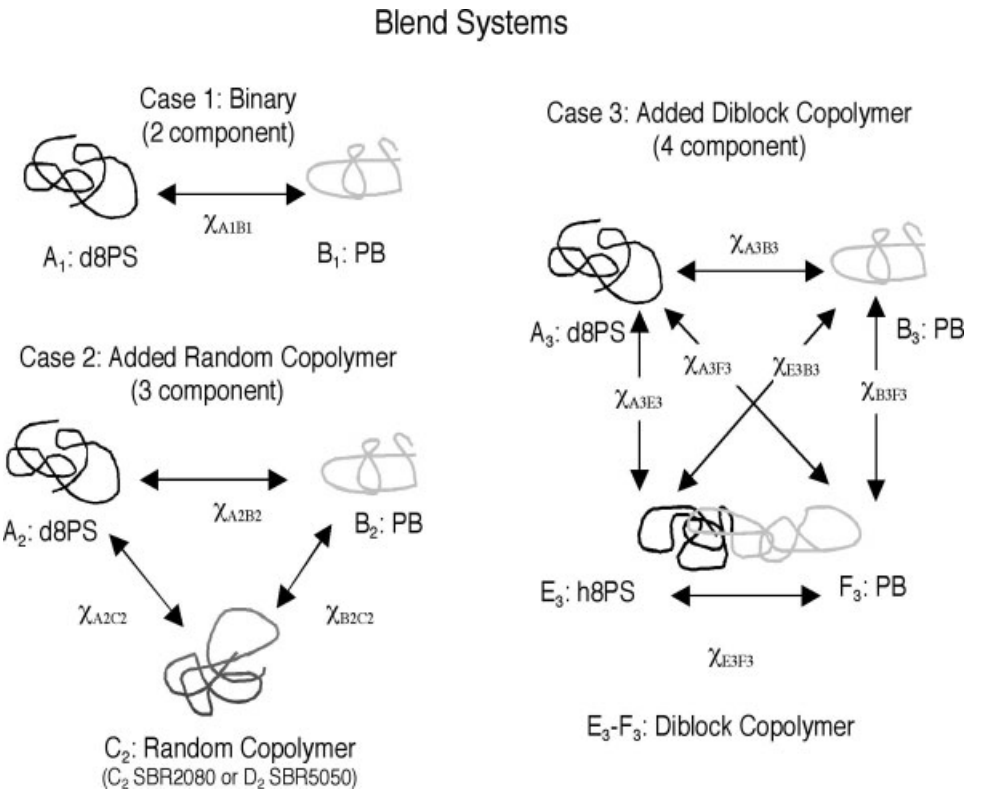

Figure 1. Depictions of the three multicomponent blend cases. A and B represent homopolymers d8PS and PB, respectively. C and D represent random copolymers SBR2080 and SBR5050, respectively. E and F represent the h8PS and PB blocks of the diblock copolymer. The subscript number is the value of $n - 1$ for the multicomponent RPA equations.

all cases, the homopolymers are always considered the last two components. Thus, in case 2, component 1 is the copolymer, whereas in case 3, components 1 and 2 are the individual blocks of the diblock. The following equations have been used for all cases for which n defines the number of components:

$$\mathbf{S}^{\circ}_{ii}(q) = N_i \phi_i \nu_i P_i(q) \; (i = 1, n-1) \tag{3a}$$

$$\mathbf{V}_{ii}(q) = \frac{1}{N_n \phi_n \nu_n P_n(q)} - \frac{2\chi_{in}}{\nu} \; (i = 1, n-1) \tag{3b}$$

$$\mathbf{V}_{ij}(\mathrm{q}) = \frac{1}{N_n \phi_n \nu_n P_n(q)} - \frac{\chi_{in}}{\nu} - \frac{\chi_{jn}}{\nu} + \frac{\chi_{ij}}{\nu} \; (\text{all } i \neq j, i < n) \tag{3c}$$

$$\mathbf{B}_i(q) = \frac{b_i}{\nu_i} - \frac{b_n}{\nu_n} \; (i = 1, n-1) \tag{3d}$$

where N_i is the degree of polymerization for the polymer, ϕ_i is the volume fraction of the blend for component i, ν_i is the volume of monomer i, and b_i is the monomer scattering length. The Flory-Huggins parameter, χ_{ij}, is between the binary pair of polymers with respect to a reference volume ν.

The single-chain structure factor $P_i(q)$ is determined with the Debye formula:

$$P_i(q) = \frac{2}{U_i}(e^{-U_i} - 1 + U_i) \text{ with } U_i = q^2 R_{gi}^2, \qquad R_{gi}^2, = \frac{N_i l_i^2}{6} \; (i = 1 \text{ to } n-1) \tag{4}$$

where R_{gi} is the radius of gyration, N_i is the number of segments, and l_{i} is the average segment length.

The off-diagonal elements of the structure factor matrix are dependent on the specific case. For cases 1 and 2, the off-diagonal elements are

Table 1. Polymer Sample Characteristics

Polymer Code	$M_w \times 10^3$	M_w/M_n	Content (%)[c]		Microstructure (%)[d]	
			W_{PS}	W_{PB}	Cis and Trans	Vinyl
d8PS	1.94	1.19	100	0	N/A	N/A
PB	2.98	1.08	0	100	92	8
SBR2080[a]	17	1.1	20	80	86	14
SBR5050[a]	68.2	3.7	51	49	73	27
SBB5050[b]	27.7	1.06	50	50	90	10

[a] Poly(styrene-*random*-butadiene).
[b] Poly(styrene-*block*-butadiene).
[c] Weight percentage of the component in the copolymer.
[d] Microstructure of the butadiene portion of the copolymer.

$$\mathbf{S}^{o}_{ij}(q) = 0 \text{ (for all } i \text{ and } j) \quad (5)$$

For case 3, the off-diagonal elements are

$$\mathbf{S}^{o}_{ij}(q) = 0 \ (i,j \neq 1, 2) \quad (6a)$$

$$\mathbf{S}^{o}_{12}(q) = \mathbf{S}^{o}_{21}(q) = (N_1\phi_1\nu_1 N_2\phi_2\nu_2)^{1/2} F_1(q)F_2(q) \quad (6b)$$

The interspecies correlations between monomers for the diblock (case 3) are nonzero, and the Leibler formula[26] [$F_i(q)$] used is

$$F_i(q) = \frac{1 - e^{-U_i}}{U_i} \ (i = 1, 2) \quad (7)$$

Blends with added random copolymers result in 2 $\times$ 2 matrices, whereas the binary polymer blend with the added diblock copolymer results in 3 $\times$ 3 matrices.

The preceding matrix equations simplify the analysis of a binary polymer blend to the more familiar binary RPA equation,[2–4] in which the total inverse intensity $I(q)$ is related to the sum of the individual inverse structure factors by the following equation:

$$\frac{k}{I(q)} = \frac{1}{N_1\phi_1\nu_1 P_1(q)} + \frac{1}{N_2\phi_2\nu_2 P_2(q)} - \frac{2\chi_{12}}{\nu} \quad (8)$$

where k is defined as

$$k = \left(\frac{b_1}{\nu_1} - \frac{b_2}{\nu_2}\right)^2 \quad (9)$$

and the variables are defined as previously discussed.

This multicomponent RPA theory has been successfully used to analyze SANS data from a number of different multicomponent polymeric systems.[27–31] For example, Hammouda et al.[27] studied a ternary polymer blend of PS, deuterated PS, and poly(vinyl methyl ether) for which Flory–Huggins interaction parameters were obtained. Also, Balsara et al.[28] studied a homopolymer blend with an added diblock copolymer over a wide range of diblock concentrations with SANS. They found that the measured Flory–Huggins interaction parameters were consistent with the concepts of the Flory–Huggins theory.

EXPERIMENTAL

Materials and Preparation

The characteristics of the polymers used in this work are summarized in Table 1. The PB homopolymers and the three copolymers were synthesized at the Goodyear Tire and Rubber Co. with anionic techniques. The deuterated PS (dPS) was prepared locally with standard anionic procedures in a positive argon pressure reactor system. The molecular weight was controlled to match the molecular weight of the PS homopolymer sample from ref. 4. The deuterated polymer was characterized via size exclusion chromatography and found to be indistinguishable from hydrogenated PS. The polymers were purified through dissolution in a solvent, filtration with a fritted filter, and filtration with a 0.45-μm Teflon filter. These procedures have been reported in detail elsewhere.[4]

The blend samples were prepared in the bulk state. The antioxidant, Goodyear Wingstay 29,

Table 2. Polymer Blend Sample Compositions

Sample Code	Volume Fraction of the Blend Components				
	d8PS	PB	SBR2080	SBR5050	SBB5050
Binary	0.776	0.224	0	0	0
R2080	0.758	0.219	0.023	0	0
R5050	0.757	0.219	0	0.024	0
B5050	0.758	0.219	0	0	0.023

was used at concentrations of 0.1% (w/w) or less. The binary and ternary blend systems were all prepared so that the d8PS and PB homopolymers were at a constant mass fraction of 0.75 for d8PS. They were heated in a vacuum oven to a temperature well above the PS glass-transition temperature, allowed to melt, mechanically mixed, and then the oven was evacuated. The samples were periodically mixed over a period of 4–6 h. The resulting blends were homogeneous.

The blend sample (heated above the phase boundary) was placed on one of the two quartz flats used in a cell. The blend sample rapidly quenched in temperature and solidified. A Teflon spacer (125 μm) was used between the two quartz flats to maintain the sample path length and seal the sample cell. The sample cell was heated until the blend softened and then the cell was compressed to seal the system.

SANS

SANS measurements were performed on the NG-3 30-m beam line at the Center for Neutron Research at the National Institute of Standards and Technology (Gaithersburg, MD). The neutron wavelength was 6.0 Å, and the sample-to-detector distance was 4.7 m. After thermal equilibration, a sample counting time of 5 min was used to acquire detector counts of approximately 10^5 or greater.

RESULTS AND DISCUSSION

Four different polymer blends were studied in the one-phase region approaching their respective phase boundaries. The compositions of the blends are listed in Table 2. The first blend is a binary blend of PS and PB; sample scattering data are shown in Figure 2. The next three blends have the same ratio of PS to PB and a low concentration

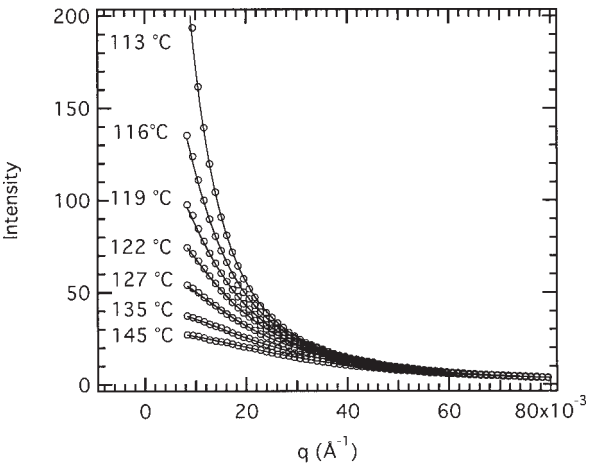

Figure 2. Neutron scattering intensity versus q for the binary blend. The scattering curves are labeled with their temperatures. The solid lines running through the data points are curve fits to the binary RPA function described in the Scattering Theory section.

[~2.5% (w/w)] of the copolymer additives (SBR2080, SBR5050, and SBB5050). Figure 3 shows scattering data for each of the blend samples at 122 °C. The binary blend is included as a reference. For the R2080 blend, the scattering is increased with respect to the binary blend. This is consistent with the SBR2080 additive reducing the miscibility and raising the (UCST) phase

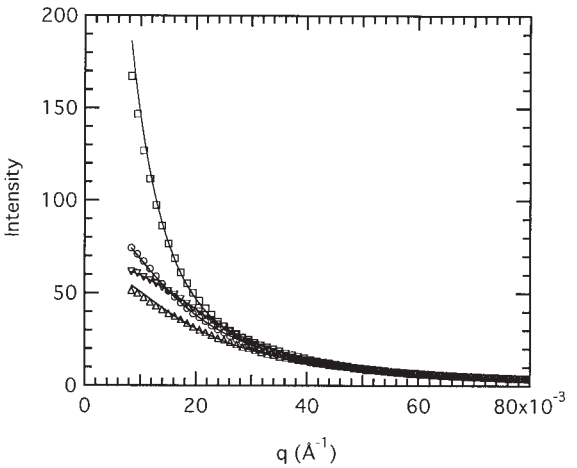

Figure 3. Neutron scattering intensity versus q for the four samples described in Table 2: (○) binary, (□) R2080, (△) R5050, and (▽) B5050. The temperature was 122 °C. The solid lines running through the data points are curve fits to the RPA functions described in the Scattering Theory section with the constraints described in the Results and Discussion section.

boundary. The R5050 and B5050 blends both have reduced scattering in comparison with the binary blend. The B5050 blend is most effective at suppressing scattering at q values lower than about 0.014 $Å^{-1}$, whereas R5050 appears to suppress scattering over all measured q values. These observations are consistent with the observations of Barham et al.,[4] who found that the R5050/B5050 blend systems showed increased miscibility, whereas the R2080 blend exhibited decreased miscibility.

Binary Blend

The scattering curves for the binary blend in Figure 2 are shown initially at high temperatures at which the blend is far from its phase boundary. As the temperature is reduced, the scattered intensity diverges at $q = 0$. The scattering data are fit to a binary RPA equation given in eq 8 with the following fitting parameters: l_i (the segment lengths of d8PS and PB are set equal to each other), the interaction parameter (χ_{A1B1}), and a background baseline. The RPA equation fits all the data very well over the measured temperature and wavevector ranges.

From the results of the fits, the intensity at zero wavevector [S(0)] has been calculated for each data set, and 1/S(0) is plotted as a function of the inverse temperature in Figure 4(a). The spinodal temperature was determined by extrapolating the higher temperature mean-field 1/S(0) data to zero, at which the curve intersects zero. The deviation from mean-field behavior occurs at about 119 °C. The vertical line connects to the zero line at the measured optical cloud point from ref. 4. The optical cloud-point temperature and the mean-field spinodal temperature are coincident and are within experimental uncertainty to the non-mean-field spinodal temperature, as shown by the dashed line (See Table 3). Figure 4(b) shows the Flory–Huggins interaction parameter obtained from the fits (χ_{A1B1}/ν) as a function of the inverse temperature. The horizontal line indicates the calculated value of the interaction parameter at the spinodal. The mean-field temperature dependence of the interaction parameter has been fit to a line, and the numerical values are listed in Table 4. The applicable temperature range and l_i values are also found in Table 4. The data from the binary system are consistent with the binary blend from ref. 4.

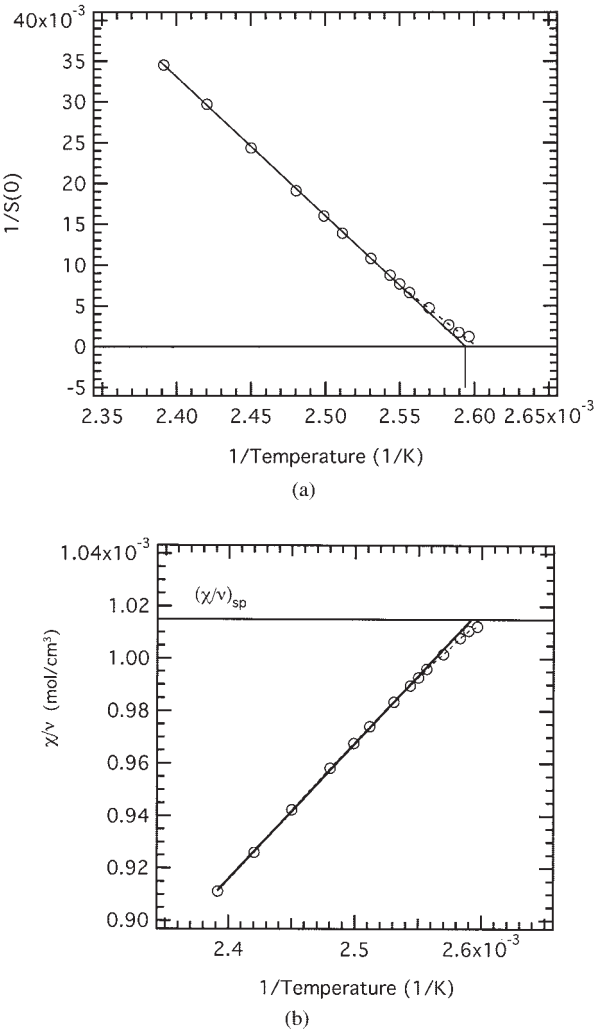

Figure 4. (a) 1/S(0) versus the inverse temperature for the binary blend. The solid line is a fit of the high-temperature data extrapolated to zero, indicating the mean-field spinodal temperature. The vertical line intersecting the zero line indicates the optical cloud point. (b) Flory-Huggins interaction parameter (χ/ν) versus the inverse temperature for the binary blend. The solid line is a fit of the high-temperature data extrapolated to the value of the interaction parameter at the spinodal.

Ternary Random Copolymer Blends

The scattering data for the two ternary blends of d8PS and PB with additives SBR2080 and SBR5050 behave qualitatively in the same manner as the binary data presented in Figure 2. The scattering data continue to increase as the temperature is lowered until the binodal is passed, and then the scattering intensity begins to diminish. The decrease in the observed scattering is due

Table 3. Phase Boundary Temperatures[a]

Sample Code	Optical Cloud Point[b]	Mean-Field Spinodal Temperature[c]	Neutron Cloud Point[d]
Binary	112.5 °C	112.5 °C	N/A
R2080	119.5 °C	120.0 °C	119.5 °C
R5050	110.0 °C	106.5 °C	109.0 °C
B5050	104.5 °C	107.0 °C	N/A

[a] All uncertainties are ± 1 °C or less.
[b] Cloud points from ref. 4.
[c] Mean-field extrapolated spinodal temperatures.
[d] Estimated binodal temperatures from upward deviations in $1/\mathbf{S}(0)$.

to phase separation and domain coalescence, with most of the domain scattering disappearing behind the beam stop at small q. This decrease in the SANS intensity for the phase-separating polymer has been observed previously.[32,33] The scattering data were initially compared with a multiple-component RPA equation given in eqs 1–7, and $n - 1$ was equal to 2. For ternary blends, there are three Flory–Huggins interaction parameters (see Fig. 1), three segment lengths, and one baseline as potential fitting parameters. The tacit assumption in this article is that the interaction parameter between the d8PS/PB interactions is equivalent to the h8PS/PB interactions, regardless of the polymer component being in the homopolymer or in a copolymer. In many blend systems, there is a measurable isotopic effect. In this particular blend case, Roe et al.[34] showed that the deuterium isotope effect is negligible. To make the analysis more tractable, the segment lengths were presumed to be equal, and the χ_{A1B1} interaction parameter from the binary data was assumed to equal the χ_{A2B2} interaction parameter between the homopolymers in the ternary blend. The other two interaction parameters, χ_{B2C2} and χ_{A2C2}, were then related to the subsequently known χ_{A1B1} interaction parameter in the manner described by Roe and others.[35–39] In this approach, the interaction parameters between the precursor homopolymers and random copolymer of the same monomers are given by the following relationships:

$$\chi_{AC} = \chi_{AB}(1 - f_A)^2 \tag{10}$$

$$\chi_{BC} = \chi_{AB} f_A^2 \tag{11}$$

where f_A is the volume fraction of monomer A in the copolymer and the labels A, B, and C refer to homopolymer A, homopolymer B, and copolymer C. With these equations, the interaction parameters for the ternary blend with the random copolymer are then all known, and the only remaining fitting parameters are the segment length and baseline. For this approach to be successful, the Flory–Huggins interaction parameter needs to be independent of the composition and such factors as the molecular architecture (i.e., χ cannot change depending on whether the monomers are in the polymer or the copolymer). The resulting RPA fit for blend sample R2080 at 122 °C with the χ values from the homopolymer blend, with only the step length and baseline varied, is shown in Figure 5 as a solid line. This approach clearly fails, and the RPA curve drastically underestimates the intensity of the scattering at a low wavevector. The results for the fitting of the R5050 blend sample were similarly unsuccessful. Other researchers have observed that χ can be a function of the chain architecture.[40–42]

To successfully fit the random copolymer ternary blends with multicomponent RPA theory, it is necessary to assume that the χ_{A2B2} interaction

Table 4. Linear Fit Parameters of χ_{AB}/ν

	$\frac{\chi_{AB}}{\nu} = a + \frac{b}{T}$ (mol/cm^3)			
Sample Code	$a \times 10^4$	b	Temperature Range (°C)[a]	l_i (Å)
Binary	−3.23 (0.09)	0.516 (0.004)	145–119	7.0 (0.1)
R2080	−1.60 (0.08)	0.411 (0.003)	145–125	7.3 (0.1)
R5050	−5.54 (0.04)	0.586 (0.002)	145–110	7.1 (0.2)
B5050	−3.45 (0.17)	0.504 (0.007)	145–116	6.9 (0.1)

[a] The temperature range was chosen to coincide with the high-temperature linear portion of the inverse susceptibility data.

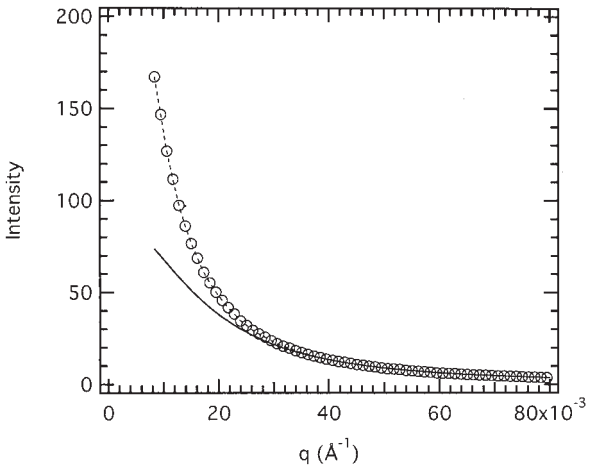

Figure 5. Neutron scattering intensity versus q for the R2080 blend. The data presented are the same R2080 data used in Figure 3, and the temperature for the data is 122 °C. The solid curve is the best fit to the data with measured interaction parameter data from the binary blend.

parameter is not equal to χ_{A1B1} and allowed to be an adjustable parameter. The other interaction parameters have been calculated from eqs 10 and 11. The segment length, the χ_{A2B2} interaction parameter, and the baseline have been adjusted in the fitting process, and all the data for both random copolymer systems can be fit with equivalent quality to the binary data. The scattering data for the R2080 sample at 122 °C are presented in Figure 3 where the solid line running through the data is the RPA fit.

Again, the intensity at S(0) has been calculated for each data set, and 1/S(0) is plotted as a function of the inverse temperature in Figure 6 for the R2080 blend and for the R5050 blend. The spinodal temperatures have been determined at the point at which the 1/S(0) data at higher (mean-field) temperatures extrapolate to zero, and they are reported in Table 3. The deviations from mean-field behavior occur at about 125 °C for the R2080 data and at about 110 °C for the R5050 data. The vertical lines connected to the zero 1/S(0) line represent the measured optical cloud points from ref. 4. In this figure, there are also two arrows that denote the binodal, as measured by SANS. The onset of the upturn in 1/S(0) has been argued to be a measure of the binodal in many literature references.[32,43] The optical cloud-point temperatures and SANS binodal temperatures agree within experimental uncertainty for both the R2080 and R5050 blends. The spinodal temperature for the R2080 blend is coincident with the SANS and optical binodal temperatures within experimental uncertainty, whereas the optical cloud-point temperature and the SANS binodal temperature for the R5050 blend are slightly higher than the spinodal temperature (see Table 3). This latter result is in contrast to that of Barham et al.,[4] who observed only a spinodal decomposition for the R5050 blend; the cloud point was coincident with the phase boundary determined from temperature jump light scattering.

Figure 6(b) shows the Flory–Huggins interaction parameters (χ_{A2B2}/ν, χ_{A2C2}/ν, and χ_{B2C2}/ν) as a function of the inverse temperature for the R2080 blend sample, and Figure 6(c) shows the same interaction parameters for the R5050 blend. The horizontal lines indicate the value of the χ_{A2B2}/ν interaction parameters at the spinodal, as calculated from the divergence of $1/\mathbf{S}(0)$. The temperature dependences of the interaction parameters for both random copolymer blend systems in the mean-field region have been fit to a linear function, and the fitted parameters are listed in Table 4. The mean-field temperature ranges and l_i values can also be found in Table 4.

Ternary Diblock Copolymer Blend

The scattering data for the B5050 blend behave qualitatively like the binary data presented in Figure 2; the scattering intensity continues to increase as the sample cools toward the phase boundary. The scattering data have been fit to the multiple-component RPA equation given in eqs 1–7; $n - 1$ is equal to 3, and each block of the diblock is considered a component. For this blend, there are now potentially six Flory–Huggins interaction parameters (see Fig. 1), four segment lengths, and one baseline for fitting parameters.

To make the fitting tractable, the segment lengths have been assumed to be equal, and the χ_{A1B1} interaction parameter from the binary data has been assumed to equal the χ_{A3B3} interaction parameter of the ternary blend. Two different initial approaches have been taken. In the first approach, all PS/PB interactions have been considered equal and equal to the interaction parameter from the binary blend ($\chi_{A1B1} = \chi_{A3B3} = \chi_{A3D3} = \chi_{A3E3} = \chi_{D3E3}$). The interaction parameter between PS and d8PS has been assumed to be equal to the values determined by Londono et al.,[44] and the interaction parameter between the PB components has been assumed to equal zero. This

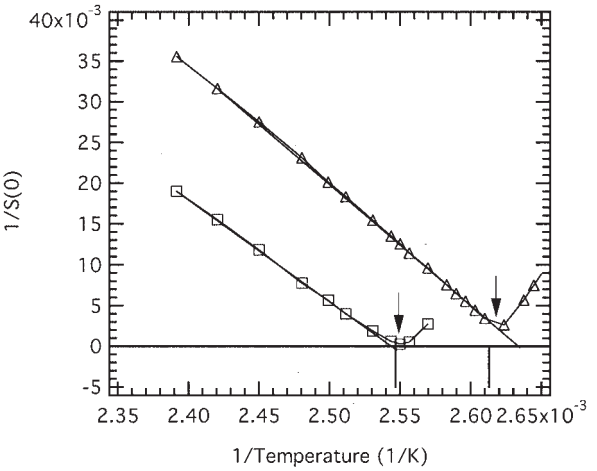

(a)

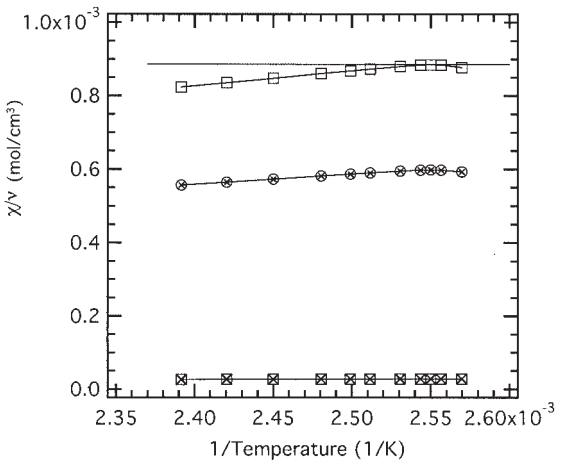

(b)

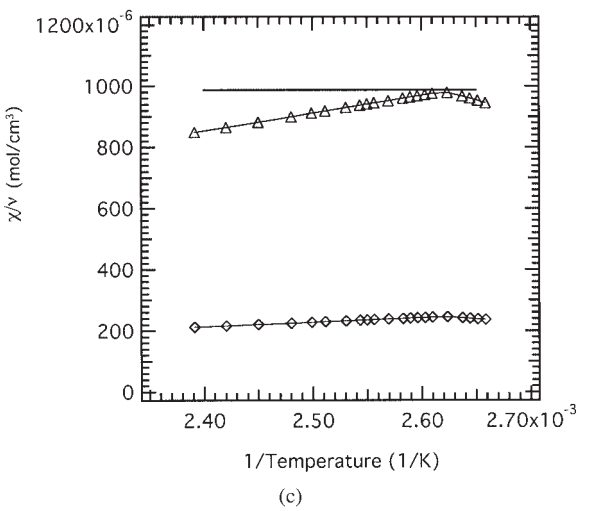

(c)

Figure 6. (a) 1/S(0) versus the inverse temperature for (□) R2080 and (△) R5050. The solid lines are fits of the high-temperature data extrapolated to zero, indicating the mean-field spinodal temperatures. The vertical lines intersecting the zero line indicate the optical cloud points. The two arrows indicate the binodal as measured by the onset of the upturn in the inverse scattering at a zero wavevector. (b) (□) χ_{A2B2}, (⊗) χ_{A2C2}, and (⊠) χ_{B2C2} versus the inverse temperature for blend R2080. The horizontal line indicates the calculated interaction parameter at the spinodal. (c) (△) χ_{A2B2}, (◇) χ_{A2C2}, and (◇) χ_{B2C2} versus the inverse temperature for blend R5050. The interaction parameters χ_{A2C2} and χ_{B2C2} are equal. The horizontal line indicates the calculated interaction parameter at the spinodal.

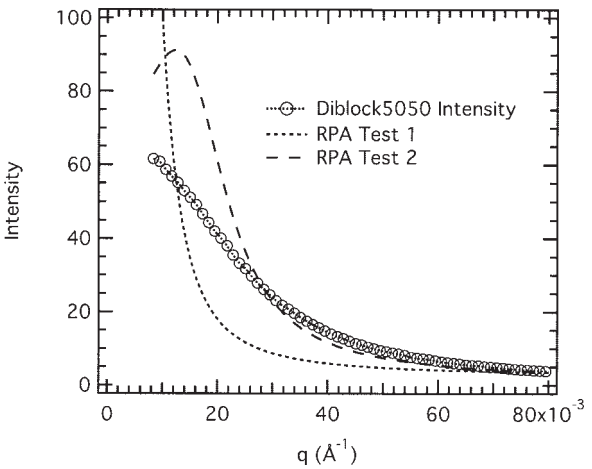

Figure 7. Neutron scattering intensity for B5050 versus q. Two test RPA fits are shown as dashed lines and are explained in the text.

approach has resulted in the curve labeled RPA Test 1 in Figure 7. In the second approach, the only change is the d8PS/PS interaction being allowed to be a fitted parameter. This result is also shown in Figure 7 and is labeled RPA Test 2. Both approaches fail in describing the correct scattering intensities. RPA Test 1 predicts much higher scattering intensities at low wavevectors and underpredicts the scattering intensities at higher wavevectors. RPA Test 2 also predicts higher intensity values at low wavevectors and predicts a peak in this vicinity while predicting roughly correct intensities at higher wavevectors.

An alternative procedure has resulted in an excellent fit of the scattering data. This fitting procedure allows the d8PS/PB interaction parameters ($\chi_{A3B3} = \chi_{A3D3}$) and the h8PS/PB interaction parameters ($\chi_{A3E3} = \chi_{D3E3}$) to be fit independently while assuming that the d8PS/h8PS interaction parameter (χ_{A3D3}) follows the data of Londono et al.[44] Figure 8(a) shows a plot of 1/S(0)

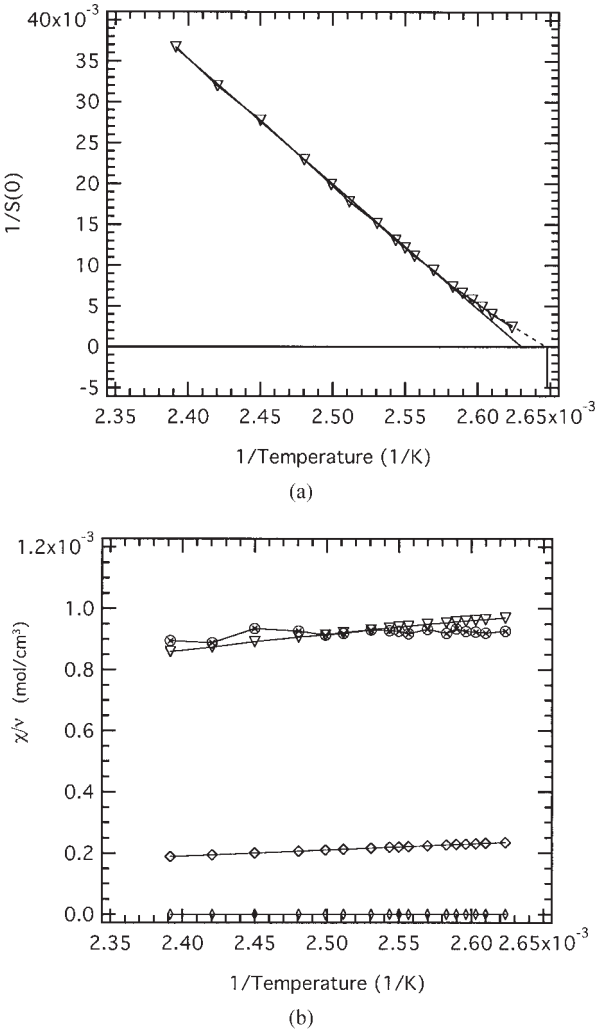

Figure 8. (a) 1/S(0) versus the inverse temperature for B5050. The solid line is a fit of the high-temperature data extrapolated to zero, indicating the mean-field spinodal temperature. The vertical lines intersecting the zero line indicate the optical cloud point. (b) χ/ν versus the inverse temperature for blend B5050: (▽) $\chi_{A3B3} = \chi_{A3F3}$, (⊗) $\chi_{E3B3} = \chi_{E3F3}$, (◇) χ_{A3E3}, and (◇) χ_{E3F3}.

versus inverse temperature. The data at higher temperatures have been fit and extrapolated to the point at which 1/S(0) intersects with zero, denoting the mean-field spinodal temperature. The vertical line, which is connected to the zero 1/S(0) line, represents the measured optical cloud point from ref. 4. Interestingly, the extrapolated 1/S(0) data for the non-mean-field critical temperature (dashed line) appear to intersect zero at the optical cloud-point temperature. Figure 8(b) contains the following interaction parameters from the fitting procedure: the h8PS/PB, the known Londono d8PS/h8PS, and the PB/PB (shown at zero). Both procedures result in identical interaction parameters between d8PS and PB (χ_{A3B3}/ν). The fitting values of the d8PS/PB interaction parameters ($\chi_{A3B3} = \chi_{A3D3}$) and the h8PS/PB interaction parameters ($\chi_{A3E3} = \chi_{D3E3}$) are equal within the uncertainties. This result is in agreement with that Roe et al.,[34] who found the deuterium isotopic effect on blends of PS and PB to be negligible.

Further Discussion

From the preceding presentation, a number of points merit emphasis. The multicomponent RPA function can be successful in fitting these data. However, a number of constraints and presumptions need to be applied. The binodal and spinodal SANS data from these blend systems corroborate well the previous light scattering data in terms of the effect that the different additives have on the equilibrium phase boundaries.

Moreover, for these data, the Flory–Huggins interaction parameter between the PS and PB homopolymers is not a unique value. Despite the intention of the original derivation of the Flory–Huggins theory, the interaction parameters are sometimes found to depend on variables such as the concentration.[45–47] To illustrate this in these data, we show the χ_{AB}/ν interaction parameters as a function of the inverse temperature for the different blend systems in Figure 9. The values of the χ_{AB} interaction parameters for all three ternary blends are reduced in comparison with the binary interaction parameter. Also included in the figure are the respective values of the mean-field interaction parameter at the spinodal, as described previously.

It is now important to revisit the initial motivation of this SANS work. The previous work by Barham et al.[4] presented two important results. The first was the discovery that the SBR5050 and SBB5050 copolymer additives both stabilized the blend, as measured by a decrease in the cloud-point data, whereas the SBR2080 additive destabilized the binary blend, as seen in the increase in the phase boundary. The general argument that is made to explain these types of results invokes changes in the interaction parameter between PS and PB. If the phase boundary temperature is reduced, then the interaction parameter is reduced because the copolymer additive lowers the interfacial tension. Conversely, when the phase boundary increases, the interaction parameter is

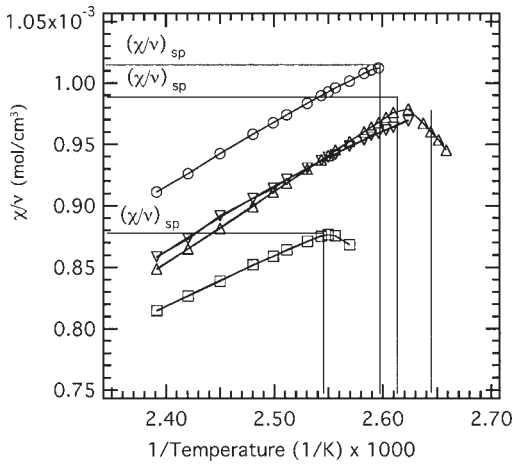

Figure 9. Flory–Huggins homopolymer A_xB_x interaction parameters versus the inverse temperature for all four blend systems: (○) binary, (□) R2080, (△) R5050, and (▽) B5050. The interaction parameters at the spinodal are indicated by horizontal lines for the binary blend (top), the R5050 blend (middle), and the R2080 blend (bottom). The vertical lines indicate the temperature of the optical cloud points for the R2080, binary, R5050, and B5050 blends from left to right.

likely increasing. Additionally, all three ternary blend systems have reduced rates of phase separation. For stabilized blend systems, it is argued that this slower rate of phase separation is a direct result of lower interfacial tension between the phases. The mean-field relationship[48,49] between the interfacial tension and the Flory–Huggins interaction parameter χ_{ij} is related through

$$\gamma_{ij} = \frac{kT}{b^2}\sqrt{\frac{\chi_{ij}}{6}} \tag{12}$$

where k is the Boltzmann constant, T is the temperature, and b is the effective length per monomer. However, if the blend with added SBR2080 is destabilized and the rate of phase separation is reduced, then these observations are in contradiction. The former appears to require an increased interaction parameter, whereas the latter appears to require a lower interaction parameter.

These contradictions can be resolved by a review of the data presented in Figure 9. First, as mentioned before, the interaction parameters between the homopolymers in the three multicomponent blend systems are lower than those in the binary blend. As a result, the interfacial tension is thus also lowered with eq 12 for all blends with additives. This in turn explains the fact that all three blend systems have slower rates of phase separation than the binary blend. Second, it is important to understand the respective decreases and increases in the temperature of the phase boundary for the three multicomponent blends. Here, two things need to be considered in concert regarding the mean-field interaction parameters: the change in the value of the interaction parameter at the spinodal for the various multicomponent blends and the absolute change in the measured values of the interaction parameters. Starting with the spinodal and measured values of the interaction parameters for the binary blend, the changes in both of these two quantities, due to the copolymer additive, become important. For the R5050 blend, the reduction in the value of the measured interaction parameter is more than the reduction of the value of the spinodal interaction parameter. The intersection of these two parameters, which defines the temperature of the spinodal, moves to a lower temperature. For R2080, the reduction of the value of the measured interaction parameter is less then the reduction of the value of the spinodal interaction parameter. In this situation, the intersection of these two lines moves to a higher temperature. Because there is not a unique value of the PS/PB interaction parameter for the B5050 blend, the spinodal is indeterminate. From the data in Figure 9 and the vertical line, which denotes the measured optical cloud point, an estimate of the spinodal interaction parameter yields a value of about 0.97 $\times 10^{-3}$ mol/cm^3. The effect of the non-mean-field behavior in the phase boundary region is small in comparison with the overall change in the interaction parameters.

CONCLUSIONS

SANS data were acquired for four d8PS/PB-based blends, with one of these being a binary blend and the other three containing one of the following additives: SBR2080, SBR5050, or SBB5050. The concentration of the added copolymers was 2.5 wt %. The resultant scattering data were fit to multicomponent RPA functions and, with appropriate constraints, fit the data very well. The temperature dependence of 1/S(0) from the four samples provided spinodal and binodal temperatures. The blend with added SBR2080 raised the phase boundary, whereas the blends with SBR5050 and SBB5050 both lowered the phase boundary. These thermodynamic results were consistent

with previous light scattering work described earlier in the article. The various Flory–Huggins interaction parameters were obtained in the mean-field region from the RPA fits. These results indicated that the Flory–Huggins interaction parameter between the PS and PB homopolymers (χ_{AB}/ν) was a function of the copolymer additive. In all cases, the blends with the copolymer additives had a reduced interaction parameter. Additionally, the value of the χ_{AB}/ν interaction parameter at the spinodal also decreased but not in concert with the decrease in the measured interaction parameter. The intersection of the measured χ_{AB}/ν interaction parameter and the spinodal value shifted consistently with the observed phase boundary changes from the extrapolated 1/S(0) data. The general reduction in the mean-field interaction parameters was also consistent with a reduction of the interfacial tensions associated with the slowing of the rate of phase separation.

These results also suggest that it is important to keep the thermodynamic effect of a phase boundary shift due to an additive distinct from the effects of changes in the interfacial tension that the additives can have on the kinetic aspect of the separation process as well as the thermodynamics of two-phase equilibrium systems. Future experiments are expected to focus on non-mean-field aspects near the phase boundary, on higher concentrations of the copolymer additives to study the applicability of multicomponent RPA to multicomponent blends, and on whether the Flory–Huggins interaction parameters become more universal at higher additive concentrations.

Support for this research from the National Institute of Standards and Technology (U.S. Department of Commerce) and the National Science Foundation [through Research in Undergraduate Institutions awards (DMR-0075968 and DMR-0314428)] is gratefully acknowledged. D. Waldow acknowledges helpful discussions with Chang-Li Yiu.

REFERENCES AND NOTES

1. Polymer Blends; Paul, D. R.; Bucknall, C. B., Eds.; Wiley: New York, 1999.
2. Utracki, L. A. Polymer Alloys and Blends; Hansen: Munich, 1989.
3. Polymer Blends; Paul, D. R.; Newman, S., Eds.; Academic: New York, 1978.
4. Barham, B.; Fosser, K.; Waldow, D.; Halasa, A. Macromolecules 2001, 34, 514.
5. Sung, L.; Han, C. C. J Polym Sci Part B: Polym Phys 1995, 33, 2405.
6. Jackson, C. L.; Sung, L.; Han, C. C. Polym Eng Sci 1997, 37, 1449.
7. Sung, L.; Nakatani, A. I.; Han, C. C.; Karim, A.; Douglas, J. F.; Satija, S. K. Phys B 1997, 241, 1013.
8. Merfeld, G. D.; Paul, D. R. Polymer 2000, 41, 649.
9. Balsara, N. P. Curr Opin Solid State Mater 1998, 3, 589.
10. Pipich, V.; Schwahn, D.; Willner, L. Appl Phys A 2002, 74, S345–S347.
11. Stepanek, P.; Morkved, T. L.; Krishnan, K.; Lodge, T. P.; Bates, F. S. Phys A 2002, 314, 411–418.
12. Morkved, T. L.; Stepanek, P.; Krishnan, K.; Bates, F. S.; Lodge, T. P. J Chem Phys 2001, 114, 7247–7259.
13. Schwahn, D.; Mortensen, K.; Frielinghaus, H.; Almdal, K.; Kielhorn, L. J Chem Phys 2000, 112, 5454–5472.
14. Schwahn, D.; Mortensen, K.; Frielinghaus, H.; Almdal, K. Phys B 1999, 82, 5056–5059.
15. Schwahn, D.; Frielinghaus, H.; Willner, L. J Chem Phys 2002, 116, 2229–2240.
16. Mortensen, K.; Almdal, K.; Schwahn, D.; Bates, F. S. J Appl Crystallogr 1997, 30, 702–707.
17. Schwahn, D.; Mortensen, K.; Frielinghaus, H.; Almdal, K. Phys Rev Lett 2000, 276, 353–354.
18. Muthukumar, M.; Huang, C. Y. J Chem Phys 1997, 107, 5561–5567.
19. Schwahn, D.; Frielinghaus, H.; Mortensen, K.; Almdal, K. Macromolecules 2001, 34, 1694–1706.
20. Schwahn, D.; Willner, L. Macromolecules 2002, 35, 239–247.
21. Frielinghaus, H.; Willner, L. Macromolecules 2001, 34, 1751–1763.
22. Akcasu, A. Z.; Klein, R.; Hammouda, B. Macromolecules 1993, 26, 4136.
23. Akcusa, A. Z.; Tombakoglu, M. Macromolecules 1990, 23, 607.
24. Hammouda, B. Adv Polym Sci 1993, 106, 87.
25. Benoit, H.; Benmouna, M.; Wu, W. L. Macromolecules 1990, 23, 1511.
26. Leibler, L. Macromolecules 1980, 13, 1602.
27. Hammouda, B.; Briber, R. M.; Barry, B. J. Polymer 1992, 33, 1785.
28. Balsara, N. P.; Jonnalagadda, S. V.; Lin, C. C.; Han, C. C.; Krishnamoorti, R. J Chem Phys 1993, 99, 10011.
29. Lin, C. C.; Jonnalagadda, S. V.; Balsara, N. P.; Han, C. C.; Krishnamoorti, R. Macromolecules 1996, 29, 661.
30. Reichart, G. C.; Graessley, W. W.; Register, R. A.; Krishnamoorti, R.; Johse, D. J. Macromolecules 1997, 30, 3363.
31. Lee, J. H.; Balsara, N. P.; Chakraborty, A. K.; Krishnamoorti, R.; Hammouda, B. Macromolecules 1996, 35, 7748.
32. Janssen, S.; Schwahn, D.; Springer, T. Phys Rev Lett 1992, 68, 3180.

33. Schwahn, D.; Mortensen, K.; Springer, T.; Yee-Madeira, H.; Thomas, R. J Chem Phys 1987, 87, 6078.
34. Lin, J. L.; Ridgy, D.; Roe, R. J. Macromolecules 1984, 18, 1609.
35. Rigby, D.; Lin, J. L.; Roe, R. J. Macromolecules 1985, 18, 2269.
36. Roe, R. J.; Zin, W. C. Macromolecules 1980, 13, 1221.
37. Scott, R. L. J Polym Sci 1952, 9, 423.
38. ten Brinke, G.; Karasz, F. E.; MacKnight, W. J. Macromolecules 1983, 16, 1827.
39. Lee, M. S.; Lodge, T. P.; Macosko, C. W. J Polym Sci Part B: Polym Phys 1997, 35, 2835.
40. Fredrickson, G. H.; Liu, A. J.; Bates, F. S. Macromolecules 1994, 27, 2503.
41. Martter, T. D.; Foster, M. D.; Yoo, T.; Xu, S.; Lizarraga, G.; Quirk, R. P. J Polym Sci Part B: Polym Phys 2003, 41, 247.
42. Martter, T. D.; Foster, M. D.; Yoo, T.; Xu, S.; Lizzaraga, G.; Quirk, R. P.; Butler, P. D. Macromolecules 2002, 35, 9763.
43. Schwahn, D.; Mortensen, K.; Yee-Madeira, H. Phys Rev Lett 1987, 58, 1544.
44. Londono, J. D.; Narten, A. H.; Wignall, G. D.; Honnell, K. G.; Hsieh, E. T.; Johnson, T. W.; Bates, F. S. Macromolecules 1994, 27, 2864.
45. Han, C. C.; Bauer, B. J.; Clark, J. C.; Muroga, Y.; Matsushita, Y.; Okada, M.; Qui, T. C.; Chang, T. H.; Sanchez, I. C. Polymer 1988, 29, 2002.
46. Wang, Z. G. J Phys 2002, 117, 481.
47. Dudowicz, J.; Freed, K. F.; Douglas, J. F. J Chem Phys 2002, 116, 9983.
48. Lee, M. S.; Lodge, T. P.; Macosko, C. W. J Polym Sci Part B: Polym Phys 1997, 35, 2835.
49. Helfand, E.; Tagami, Y. J Polym Sci Part B: Polym Lett 1971, 9, 741.